

Article

Influence of Fatigue Crack Formation and Propagation on Reliability of Steel Members

Peter Koteš *  and Josef Vičan 

Department of Structures and Bridges, Faculty of Civil Engineering, University of Zilina, Univerzitna 8215/1, 010 26 Zilina, Slovakia; josef.vican@uniza.sk

* Correspondence: peter.kotes@uniza.sk

Abstract: During the years of bridge exploitation, many degradation processes and external influences attack its structure. Therefore, bridge reliability and durability is decreasing in time. On the other hand, the traffic load remains almost the same or even higher than in the past. However, bridges should not to become the limiting component of communication capacity and traffic reliability. Regarding to reliability, bridges should be assessed from the viewpoint of the Ultimate Limit States (ULS) and Serviceability Limit States (SLS). Within the ULS, cross-sections and members are verified for various types of stressing and their combinations, and also for fatigue at the same time. The cross-sectional verification, e.g., for bending stresses and fatigue, is done independently according to corresponding criteria of the ULS determined for strength verification a fatigue assessment separately. The presented article deals with the steel railway plate girder bridge with bottom member deck, in which there is an effort to prove the effect of the crack in tension bottom flange due to fatigue stressing on the change of bending resistance over time. The analytical calculation was derived and at the same time, the probabilistic approach of the influence of the fatigue crack size on the change of the cross-sectional resistance and reliability over time was used.



Citation: Koteš, P.; Vičan, J. Influence of Fatigue Crack Formation and Propagation on Reliability of Steel Members. *Appl. Sci.* **2021**, *11*, 11562. <https://doi.org/10.3390/app112311562>

Academic Editor: Mariusz Jaśniok

Received: 17 November 2021

Accepted: 1 December 2021

Published: 6 December 2021

Publisher's Note: MDPI stays neutral with regard to jurisdictional claims in published maps and institutional affiliations.



Copyright: © 2021 by the authors. Licensee MDPI, Basel, Switzerland. This article is an open access article distributed under the terms and conditions of the Creative Commons Attribution (CC BY) license (<https://creativecommons.org/licenses/by/4.0/>).

Keywords: steel bridge; fatigue; crack growth; reliability approach; steel members; crack propagation effects

1. Introduction

Many various factors influence the bridge members during the lifetime, which can affect the change of member reliability in the time. Apart from e.g., change of loads or intensity of loads in time, which can induce a loss or growth of the reliability depending on the increase or decrease of loads, the degradation of materials significantly influences the cross-sectional reliability [1]. Therefore, it is possible to say that this factor explicitly causes the reduction of reliability of steel bridge members [2,3].

The most known ways of degradation of a steel member are corrosion of steel and fatigue processes [4–10]. Verifying structure in terms of fatigue is an inseparable part of the new structural design or part of verifying the existing bridge structures [11–15]. An increase of crack due to fatigue damage changes the member cross-sectional characteristics, as decreasing in cross-sectional area, a second moment of area and section modulus. It causes lower flexural or shear stiffness, decrease of resistance, an increase of deformations, therefore, modification of member's reliability in the time [16–18].

Bridges are heavily stressed by traffic. In the case of steel bridges, this load causes significant fatigue stresses [19–21], which can result in fatigue cracks in the tensile areas over time [22,23]. However, it is not yet known how fatigue cracks can affect e.g., cross-sectional bending resistance of the element within the time, because the verifications of the cross-sectional resistance and fatigue strength are independent assessments. From the viewpoint of ULS, the cross-sectional or member resistance, respectively, is verified according to individual criteria defined by corresponding ULS given in standards. Standard fatigue assessment of steel bridge member according to [24] is based on the comparison of

the damage equivalent stress range $\Delta\sigma_{E2}$ to the fatigue strength given in [25] in accordance with the corresponding bridge structural detail. Damage equivalent stress range should be calculated using the reference stress range $\Delta\sigma_p$ and the damage equivalence factor λ , which determination is given in [24] for railway and road bridges separately. The verification is done for determined bridge lifetime, so that this assessment does not reflect the change of structural member resistance in time due to crack growth.

The fatigue cracks on tension flange of steel structure have been an issue since the beginning of steel bridge design activities. The objective has been to use such preventive activities that would eliminate gradual growth and propagation of cracks resulting in considerable deterioration of reliability of the bridge. Though more and more advanced modifications and control methods have been introduced, the cracks still appear. The standard [25] makes it possible to use a damage tolerance method as an alternative under certain conditions. Methods proposed include the observation of a “critical” crack [26]. That term, however, has not been defined for real welded structural elements. It is hardly possible in practice to use a small test sample for direct application [27,28].

In connection with the fatigue damage of components, the design method is very important. If the ULS for fatigue are applied when designing elements in terms of design effects of the traffic load, the verification is done for the real traffic load throughout the designed service life. The acceptable size of the fatigue crack should be such so that the bridge superstructure might, at the end of its service life, still provide the required level of reliability. The tension flanges are the most stressed elements of the superstructure. Therefore, the standardized level of reliability for fatigue is determined for the tension elements.

The paper is focused on the influence of crack formation and propagation due to fatigue on the change of steel member’s reliability from the viewpoint of the Ultimate Limit States (ULS) in time. Because the work is focused on member where a measurable crack has already appeared and has propagated (grew), the linear elastic fracture mechanics (LEFM) was considered.

2. Fatigue Crack Formation and Propagation

According to [29,30], the cracks are divided into cracks propagating from the edge, from the corner, embedded cracks and cracks propagating from the surface in terms of engineering structures. The cracks usually develop in members subjected to bending or tension. Concerning the eventual broad scope of this problem, the work in the paper is limited and focused just on cracks propagating from the surface (see. Figure 1). According to Figure 1, the maximum crack depth “a” may theoretically be equal to the flange thickness “t” and the crack width 2.c may be equal to the flange width b, but the limiting conditions used are given later in paragraph 6 (Equation (29)). Cracks from the surface most often occur when the flange is e.g., joined in several parts by welds or has any defect.

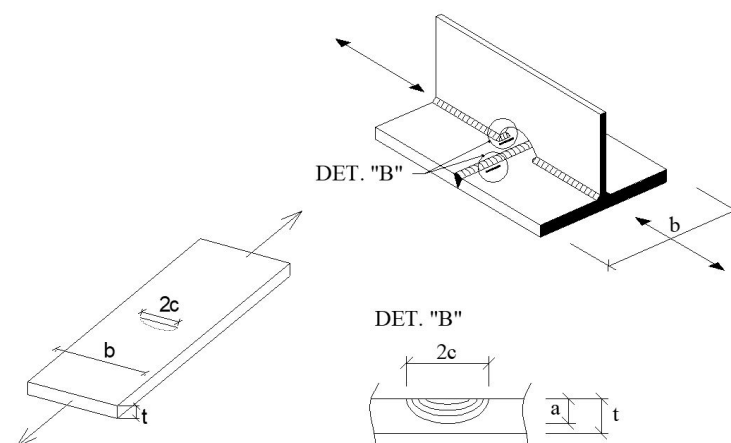


Figure 1. Crack propagated from surface.

3. Crack Propagation from Surface

State of stresses (tightness) surrounding crack tip is formulated by the stress-intensity factor (SIF) [31,32], whose value is depending on the way of stressing, size and shape of a crack and on geometry of a member. In the case of a surface crack, the model of crack propagation is more complicated than in the case of crack propagating from the edge or the embedded crack. SIF is given by Equation, which follows from superposition of tensile and bending stressing

$$K_I = \sqrt{\pi \cdot a} \cdot (\sigma_m \cdot F(a)_m \cdot M(a)_m + \sigma_b \cdot F(a)_b \cdot M(a)_b) \tag{1}$$

where:

K_I is the stress-intensity factor (SIF),

σ_m is the tensile (membrane) stress,

σ_b is the bending stress,

$F(a)_m$ is the boundary-correction factor of stress intensity for tension stress,

$F(a)_b$ is the boundary-correction factor of stress intensity for bending stress,

$M(a)_m$ is the curve-fitting function taking into account the nonlinear stress peak due to the tension effects,

$M(a)_b$ is the curve-fitting function taking into account the nonlinear stress peak due to the bending effects.

Type of crack (real shape) is substituted (e.g., according to [33]) by the semi elliptical surface crack (Figure 2) with depth of crack “a” (length of semi-axis) and half of crack width in plate surface “c” (length of the second semi-axis). “ T_{cr} ” means center of crack gravity and “ e_{cr} ” means distance of center of crack gravity from surface (eccentricity).

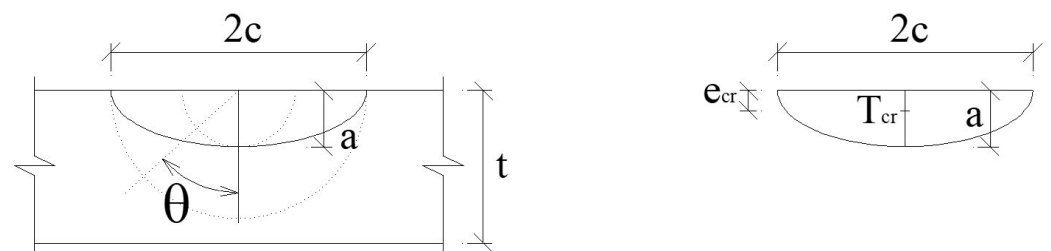


Figure 2. Shape and dimensions of a crack propagating from surface.

The change of crack cross-sectional area, depending on number of cycles N , is given by Equation

$$A_{tr}(N) = \frac{1}{2} \cdot \pi \cdot a(N) \cdot c(N) \text{ [m}^2\text{]}. \tag{2}$$

Distance of the crack center of gravity from the surface is equal to

$$e_{tr}(N) = \frac{4 \cdot a(N)}{3 \cdot \pi} \text{ [m]}, \tag{3}$$

and second moment of area is described by equation

$$I_{y,tr}(N) = \left(\frac{\pi}{8} - \frac{8}{9 \cdot \pi} \right) \cdot a(N)^3 \cdot c(N) \text{ [m}^4\text{]}. \tag{4}$$

In the case of the crack propagating from surface, it is not enough to investigate the change of just one crack dimension during crack form changing and its increasing, what is in the case of crack propagating from the edge or from the middle. It is necessary to take into account the change of both dimensions “a” and “c” in both semi-axes directions. The

stress-intensity factor K_I for semi-elliptical surface crack propagating from the surface in a slab member subjected to tension and bending has the basic form [34,35]

$$K_I = F(a) \cdot \sqrt{\frac{\pi \cdot a}{\Phi}} \cdot (\sigma_m + H \cdot \sigma_b), \quad (5)$$

where:

$F(a) = F(a/t, a/c, 2c/b)$ is the boundary-correction factor for surface crack in a plate,
 a, b, c, t, θ are the geometrical parameters of a member and a crack (Figures 1 and 2),

a is the crack depth,

c is the half of the crack width,

b is the width of the cracked plate,

t is the thickness of the cracked plate,

θ is the parametric angle of ellipse,

H is the function expressing change of $F(a)$ in the case of bending stressing,

Φ is the shape factor for an elliptic crack, where

$$\Phi = \int_0^{\pi/2} \left[\left(\frac{a}{c} \right)^2 \cdot \sin^2 \theta + \cos^2 \theta \right]^{0.5} d\theta. \quad (6)$$

One of the most used empirical Equation for Φ was derived in [36] and it depends on ratio between the crack depth “ a ” and half of crack width “ c ”

$$\Phi = 1 + 1.464 \cdot \left(\frac{a}{c} \right)^{1.65}, \quad \text{for } \frac{a}{c} \leq 1, \quad (7)$$

$$\Phi = 1 + 1.464 \cdot \left(\frac{c}{a} \right)^{1.65}, \quad \text{for } \frac{a}{c} > 1. \quad (8)$$

In general, it is possible to write the boundary-correction factor $F(a)$ in the following form

$$F(a) = M \cdot S = \left[M_1 + M_2 \cdot \left(\frac{a}{t} \right)^2 + M_3 \cdot \left(\frac{a}{t} \right)^4 \right] \cdot S, \quad (9)$$

where M_i are the curve-fitting functions,

$$M_1 = 1.13 - 0.09 \cdot \left(\frac{a}{c} \right), \quad (10)$$

$$M_2 = -0.54 + \frac{0.89}{0.2 + \left(\frac{a}{c} \right)}, \quad (11)$$

$$M_3 = 0.5 - \frac{1}{0.65 + \left(\frac{a}{c} \right)} + 14 \cdot \left(1 - \frac{a}{c} \right)^{24}, \quad (12)$$

$$S = g \cdot f_\phi \cdot f_w, \quad (13)$$

where:

g is the fine-tuning curve-fitting function,

f_ϕ is the angular function derived from embedded elliptical crack solution,

f_w is the finite-width correction,

and it is valid for $\frac{a}{c} \leq 1$

$$g = 1 + \left[0.1 + 0.35 \cdot \left(\frac{a}{t} \right)^2 \right] \cdot (1 - \sin \theta)^2, \quad (14)$$

$$f_\phi = \left[\left(\frac{a}{c} \right)^2 \cdot \sin^2 \theta + \cos^2 \theta \right]^{1/4}, \quad (15)$$

$$f_w = \left[\sec\left(\frac{\pi \cdot c}{b} \cdot \sqrt{\frac{a}{t}}\right) \right]^{1/2}, \quad f_w = 1 \text{ is valid for the large crack width.} \quad (16)$$

If the focus is on biaxially symmetric welded steel I-beams and one assumes that there is a crack in the tension bottom flange (positive moment), then we can neglect the gradient of bending stress through flange thickness. In that case, it could be considered that the flange is subjected only to axial tensile force, from which it is stressed only by tensile (membrane) stress $\sigma_m = \sigma$. Then, it is possible to simplify Equation (5) into form

$$K = F(a) \cdot \sqrt{\frac{\pi \cdot a}{\Phi}} \cdot \sigma. \quad (17)$$

However, this assumption should be only applied to thin flanges. In the case of thick flanges according to literature [35], the influence of the normal stress gradient on the thickness of the flanges is positively affected. In the case of longitudinal girders, the thickness of flanges varies from 10 mm to 25 mm as maximum, whereas minimum height of longitudinal girder is 500 mm. The thickness of cross-girder flanges varies from 20 mm to 30 mm, whereas the cross-girders heights are minimum of 700 mm.

4. Fatigue Crack Propagation

In general, the rate of fatigue crack growth is given as the derivation of crack depth “a” with respect to number of loading cycles “N”. It means that it is ratio da/dN . For simplification, the constant range of the nominal stress $\Delta\sigma$ is considered. Then, for a given crack depth and constant stress range $\Delta\sigma$ one can plot the values $\log da/dN$ in terms of $\log \Delta K$, where ΔK is the SIF (stress-intensity factor) range

$$\Delta K = K_{\max} - K_{\min} = F(a) \cdot \Delta\sigma \cdot \sqrt{\frac{\pi \cdot a}{\Phi}}. \quad (18)$$

Dependence of $\log (da/dN)$ on $\log \Delta K$ is approximately linear and is expressed by the Paris-Erdogan law

$$\frac{da}{dN} = C \cdot (\Delta K)^m, \quad (19)$$

where:

da/dN is the change in the length of the fatigue crack per load cycles,

ΔK is the interval (range) of the stress intensity factor (SIF),

C , m are the material constants,

N is the number of loading cycles.

The material constants C and m are empirical constants, which are functions of the material properties and microstructure and are obtained experimentally and also usually depend on environment, fatigue frequency, temperature and mean stress or load ratio, loading mode, stress state, where m is the slope of the curve showing the rate of crack propagation according to the Paris-Erdogan equation in the mean linear region (on a logarithmic scale). The upper limit for $C = 6.89 \cdot 10^{-12} \text{ MPa}^{-3} \cdot \text{m}^{-1/2}$ (in the case of the use of millimeters $2.18 \cdot 10^{-13} \text{ MPa}^{-3} \cdot \text{mm}^{-1/2}$) is used and $m = 3$ for structural steels in the case of tensile cracks.

Paris-Erdogan' law is a crack growth equation that gives the rate of growth of a fatigue crack. The stress intensity factor K characterizes the load around a crack tip and the rate of crack growth is experimentally shown to be a function of the range of stress intensity ΔK seen in a loading cycle. The stress intensity factor, K , is used in fracture mechanics to predict the stress state (“stress intensity”) near the tip of a crack or notch caused by a remote load or residual stresses [37]. P. C. Paris introduced the idea that the rate of crack growth may depend on the stress intensity factor [38] in a year 1961. Then in their 1963 paper [39], Paris and Erdogan indirectly suggested the equation with the aside remark “The authors are hesitant but cannot resist the temptation to draw the straight line slope 1:4 through the

data" after reviewing data on a log-log plot of crack growth versus stress intensity range. The Paris equation was then presented with the fixed exponent of 4.

5. Effect of Crack on Steel Member's Reliability

In the engineering probability method, the reliability margin $g(R,E) = G$ is given by Equation

$$g(R,E) = G = R - E, \quad (20)$$

where:

R is the random variable resistance of a structural member,
 E is the random variable load effects of the same element.

It is assumed that the member resistance R is normally distributed random variable $N(m_R, s_R^2)$ and that the load effects E are also normally distributed $N(m_E, s_E^2)$, where is valid that R and E are mutually independent. The normally distributed random variables R and E are given by the mean values (m_R, m_E) and the standard deviations (s_R^2, s_E^2).

The member's reliability is given either by the failure probability P_f or by reliability index β . If one considers the change of member resistance $R(N)$ in time t due to fatigue damage (crack formation and development depending on cycles number N), then the reliability of the member is also changing in time, it follows that the failure probability $P_f(N)$ and reliability index $\beta(N)$ are also varying in time t .

As was mentioned, the paper is focused on the welded steel biaxially symmetric I-beam subjected to bending. In this case, the member's resistance $R(t)$ for compact and semi compact cross-sections is given by the equation

$$R(N) = M(N)_{pl,y} = f_y \cdot W(N)_{pl,y}, \quad [\text{kNm}] \text{ for cross-sections of class 1 and 2,} \quad (21)$$

$$R(N) = M(N)_{el,y} = f_y \cdot W(N)_{el,y,dol}, \quad [\text{kNm}] \text{ for cross-sections of class 3,} \quad (22)$$

where:

f_y is the random variable yield strength of structural steel [MPa],

$W(N)_{pl,y}$ is the time dependent random variable plastic section modulus [m^3],

$W(N)_{el,y}$ is the time dependent random variable elastic section modulus [m^3].

That theoretical approach does not consider the cross-sections of class 4. In the case of compact cross-section 1 and 2, the time dependent plastic section modulus $W(N)_{pl,y}$ taking into account the cross-section loss due to crack development is represented by the relation

$$W(N)_{pl,y} = b_f \cdot t_f \cdot \left(d - e_1^*(N) + \frac{t_f}{2} \right) + \frac{t_w}{2} \cdot \left[(d - e_1^*(N))^2 + (e_1^*(N))^2 \right] + [b_f \cdot t_f - 0.5 \cdot \pi \cdot a(N) \cdot c(N)] \cdot \left[e_1^*(N) + \frac{b_f \cdot t_f^2 - \pi \cdot a(N) \cdot c(N) \cdot \left(t_f - \frac{4 \cdot a(N)}{3 \cdot \pi} \right)}{2 \cdot b_f \cdot t_f - \pi \cdot a(N) \cdot c(N)} \right] \quad (23)$$

where

$$e_1^*(N) = \frac{d}{2} + \frac{\pi \cdot a(N) \cdot c(N)}{4 \cdot t_w}, \quad (\text{shows the change of cross-sectional centre of gravity}). \quad (24)$$

Meaning of each cross-sectional characteristics is shown in Figure 3.

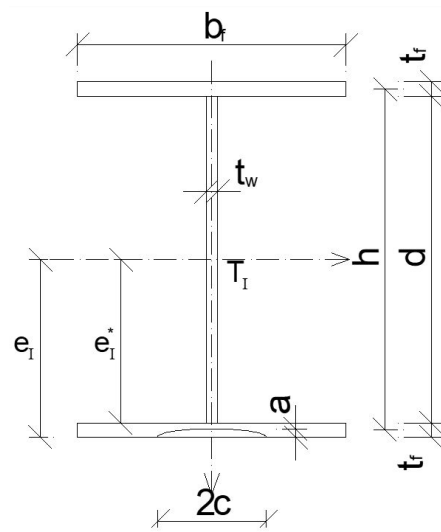


Figure 3. Cross-sectional characteristics of biaxially symmetric I-beam.

Similarly, the time dependent elastic section modulus $W(N)_{el,y}$ of the cross-sections of class 3 taking into account the cross-section loss of the flange due to crack development is given by Equation

$$W(N)_{el,y,hor} = \frac{I(N)_y}{d + t_f - e_I^*(N)}, \text{ for the upper fibres of cross-section,} \quad (25)$$

$$W(N)_{el,y,dol} = \frac{I(N)_y}{t_f + e_I^*(N)}, \text{ for the bottom fibres of cross-section,} \quad (26)$$

where the second moment of area is calculated according to

$$I(N)_y = \frac{1}{6} \cdot b_f \cdot t_f^3 + b_f \cdot t_f \cdot \left[\left(\frac{t_f}{2} + d - e_I^*(N) \right)^2 + \left(\frac{t_f}{2} + e_I^*(N) \right)^2 \right] + \frac{1}{12} \cdot t_w \cdot d^3 + t_w \cdot d \cdot \left(e_I^*(N) - \frac{d}{2} \right)^2 - \frac{\pi}{8} \cdot a^3(N) \cdot c(N) - \frac{\pi}{2} \cdot a(N) \cdot c(N) \cdot \left(e_I^*(N) + t_f - \frac{4 \cdot a(N)}{3 \cdot \pi} \right)^2, \quad (27)$$

where in this case

$$e_I^*(N) = \frac{b_f \cdot t_f \cdot (d + 2 \cdot t_f) + d \cdot t_w \cdot \left(\frac{d}{2} + t_f \right) - \frac{2}{3} \cdot a^2(N) \cdot c(N)}{2 \cdot b_f \cdot t_f + d \cdot t_w - \frac{\pi}{2} \cdot a(N) \cdot c(N)} - t_f. \quad (28)$$

Since the dependence of crack depth “a” and half of crack width “c” growth on cycles number N (a(N), c(N)) is not known yet, they are considered in equations as independent on cycles number N with denotations “a(N) = a” and “c(N) = c”.

6. Independent Crack Growth in Directions “a” and “c”

In the first case, one focuses on the independent growth of a crack in the direction of the two half-axes (depth and width). In that case, the dimensions “a” and “c” are independently chosen from each other. From that follows, that the chosen cracks have different shapes (different ellipses) and the different areas.

6.1. Analytical Calculation

To determine the influence of the size and shape of fatigue crack on the cross-sectional resistance, the parametric study was performed [40,41]. The welded steel beam I 400, representing, for example, longitudinal girder of steel plate girder bridge with a bottom members’ deck (Figure 4) and I 800, representing cross girder of the same bridge, were considered in the study. The input strength and geometric characteristics are shown in

Table 1. The length of the bridge is 30.0 m. The lengths of the longitudinal girders of plate girder railway bridges vary about (1.6–2.5) m. In the case of railway bridge cross-girders, their lengths are 5.5–6.5 m depending on the bridge arrangement.

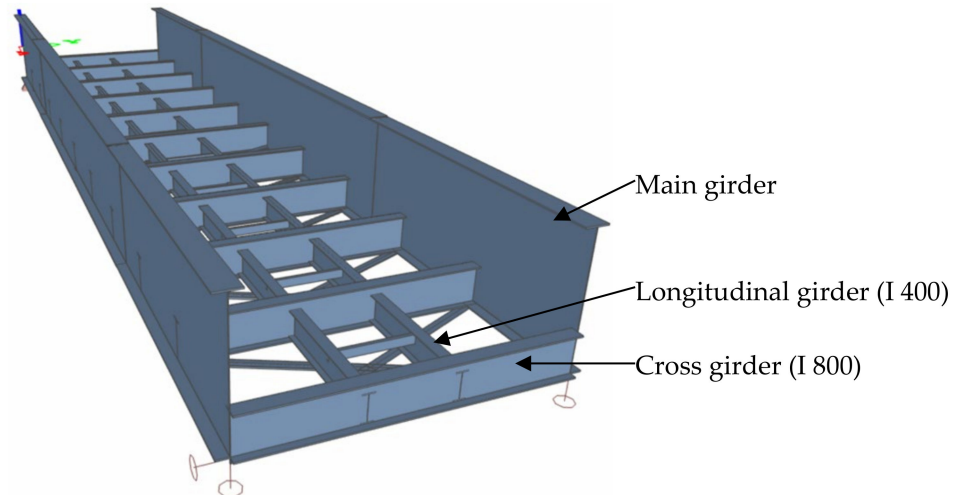


Figure 4. Model of typical steel plate girder bridge with bottom member members' deck on railway line Žilina-Martin with girders I 400 and I 800 used in parametric study.

Table 1. Cross-section characteristics of welded steel beams I 400 and I 800.

Input Characteristics	I 400	I 800
Yield strength— f_y [MPa]	235.0/1.0 = 235.0	235.0/1.0 = 235.0
Flange width— b_f [mm]	100.0	250.0
Flange thickness— t_f [mm]	10.0	25.0
Web height— d [mm]	380.0	750.0
Web thickness— t_w [mm]	8.0	10.0

Since this is a cross-section of class 1 (I 400) and class 2 (I 800), the Equations (21) and (23) were used for cross-sectional resistance calculation. The results of crack growth influence on plastic section modulus $W_{pl,y}$ decreasing are shown in Figure 5, and on plastic bending resistance $M_{pl,y}$ are shown in Figure 6.

Crack size was chosen from a minimum value (zero value) up to the size defined by the limit values

$$2 \cdot c \leq 0.8 \cdot b_f, \text{ and } a \leq 0.8 \cdot t_f. \quad (29)$$

For I 400, the limit values are $2 \cdot c \leq 0.8 \cdot 0.100 = 0.080$ m and $a \leq 0.8 \cdot 0.010 = 0.008$ m, for I 800 the limit values are $2 \cdot c \leq 0.8 \cdot 0.250 = 0.200$ m and $a \leq 0.8 \cdot 0.025 = 0.020$ m.

From the results obtained, it can be seen that the fatigue crack growth can largely reduce the moment load-carrying capacity. If the maximum possible crack from surface limited by conditions (29) would appear, it would lead to the cross-sectional area loss of 9.97% (I 400), 15.71% for I 800, while the plastic resistance moment would be reduced up to 33.77% (I 400), 55.15% (I 800) respectively.

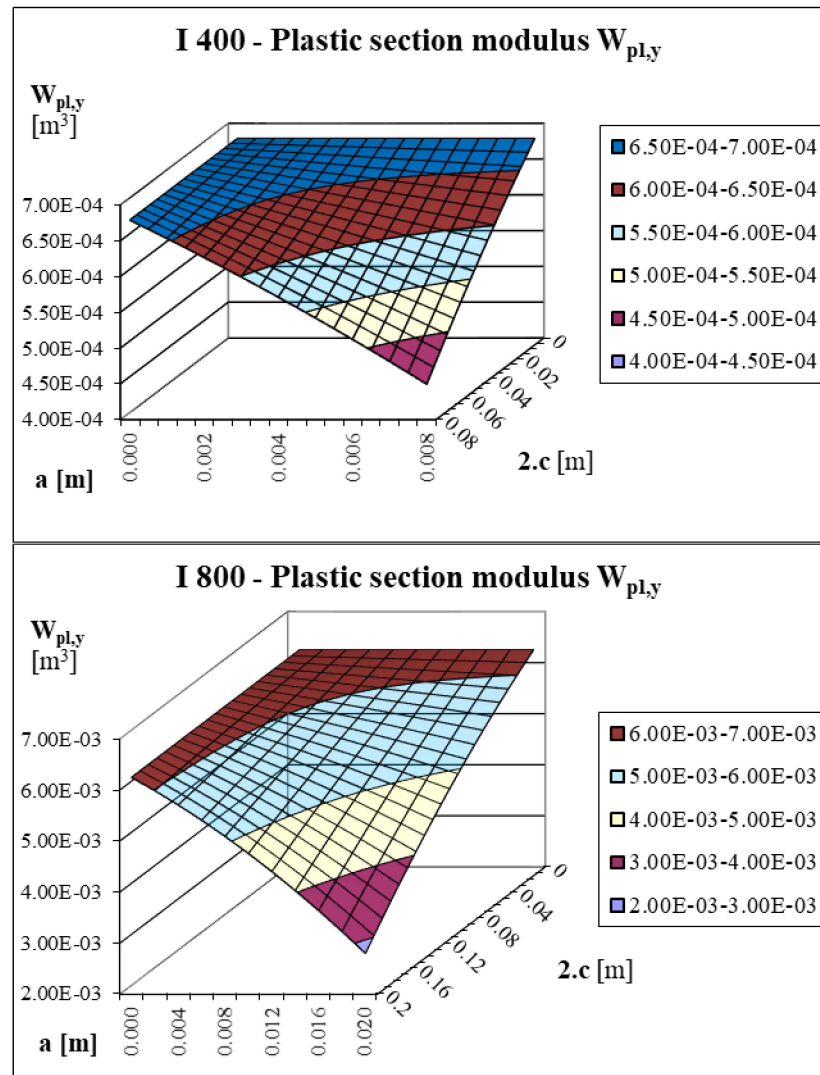


Figure 5. Influence of crack size on plastic section modulus $W_{pl,y}$.

6.2. Probabilistic Approach

The probabilistic approach was used for finding the impact of fatigue crack on failure probability variation and on corresponding reliability index [42]. In that case, all strength and geometrical characteristics were considered as random variables with normal distribution $N(m,s^2)$ and they are shown in Table 2 [43,44]. The steel of quality S235 was assumed. Statistical characteristics of yield strength were taken from [45]. Likewise, all geometric characteristics (thickness and width) of plates were taken from [45]. Standard deviations, reflecting tolerances of flange widths, take into account the deviations allowed by standard [46]. Dimensions of crack semi-axes (c,a) were again chosen and were considered as constants, not as random variables. Numerical application of resistance calculation $R = M_{pl,y}$ was realised using the simulation method Monte-Carlo.

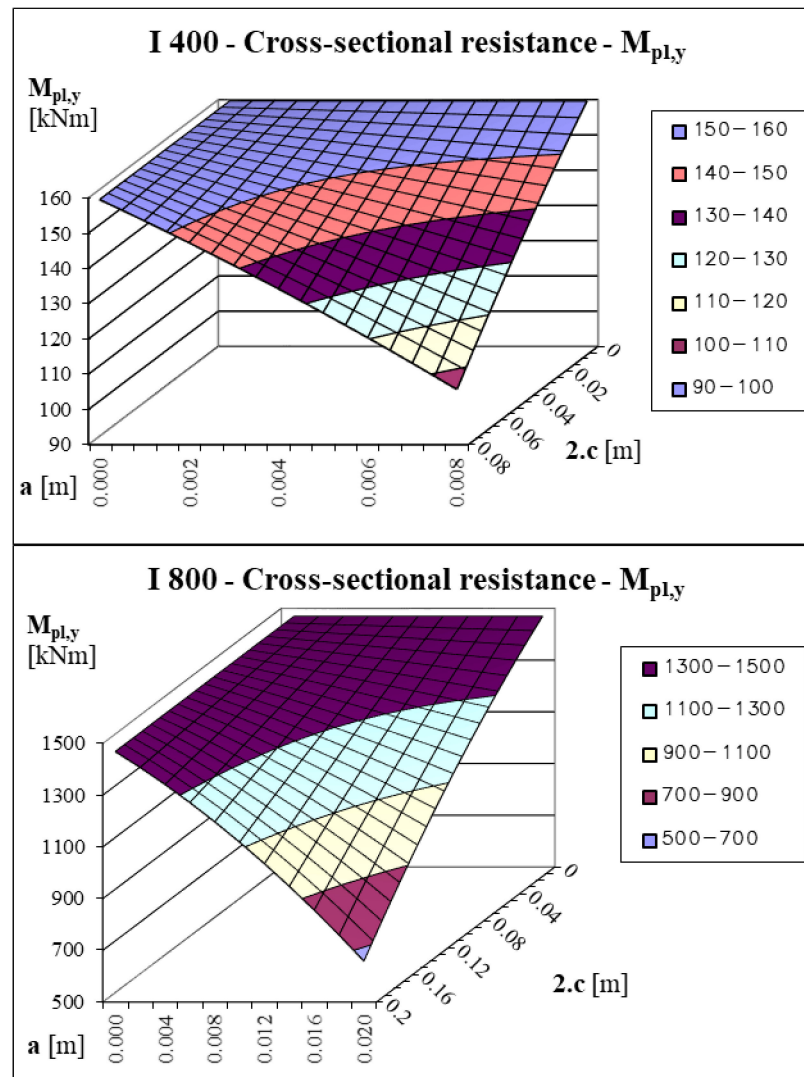


Figure 6. Influence of crack size on plastic resistance moment $M_{pl,y}$.

Table 2. Statistical characteristics of welded steel beams I 400 and I 800.

Input Characteristics	I 400-Welded			I 800-Welded			Probability Distribution
	m	s	v	m	s	v	
Yield strength— f_y [MPa]	269.20	28.00	0.104	281.00	27.80	0.099	Normal
Flange width— b_f [mm]	100.00	2.00	0.020	250.00	2.00	0.008	Normal
Flange thickness— t_f [mm]	10.210	0.37	0.036	25.525	0.925	0.036	Normal
Web height— d [mm]	380.00	2.00	0.005	750.00	2.00	0.003	Normal
Web thickness— t_w [mm]	8.168	0.296	0.036	10.210	0.37	0.036	Normal

Obtained results of mean value m_R and standard deviation s_R variation are shown in Figures 7 and 8. As expected, the results show detectable decrease of the mean value m_R and standard deviation s_R . This is the proof that influence of fatigue crack development and propagation may have unavoidable influence on member resistance. In this case, the mean value of resistance m_R was decreased by a maximum 15.33% (I 400) and 19.54% (I 800) and the standard deviation s_R was decreased by a maximum 12.73% (I 400) and 18.73% (I 800).

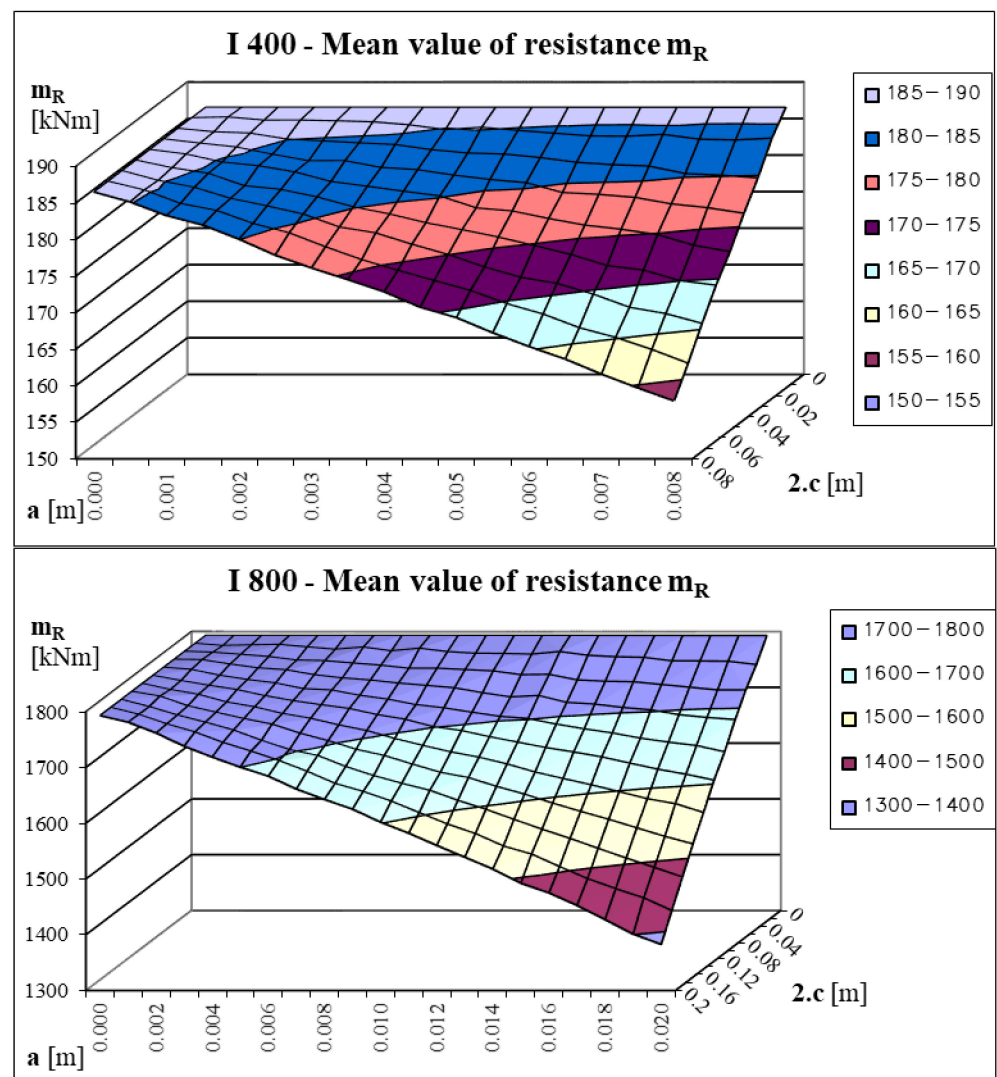


Figure 7. Influence of crack size on resistance mean value m_R .

The consequential obtained values of parameters are

$$\text{I 400: } m_R = 186.515 \text{ kNm, I 800: } m_R = 1792.906 \text{ kNm,}$$

$$s_R = 20.176 \text{ kNm, } s_R = 186.036 \text{ kNm}$$

The load effects E were considered as random variables normally distributed with the following parameters

$$\text{I 400: } m_E = 94.411 \text{ kNm, I 800: } m_E = 943.651 \text{ kNm,}$$

$$s_E = 15.132 \text{ kNm, } s_E = 139.527 \text{ kNm.}$$

From parameters follows that members were designed with reliability index $\beta = 3.652$ for design lifetime $T_d = 100$ years. The results of crack growth influence on failure probability P_f and reliability index β are shown in Figures 9 and 10.

Decrease of the mean value m_R causes decrease of the member's—decrease of reliability index β and corresponding increase of failure probability P_f . Decrease of the standard deviation, in general, has favourable influence on members' reliability (the failure probability P_f is lower in time). Since the results show a decrease of the reliability, it follows that the reliability is mainly influenced by the decrease of the mean value m_R . The decrease of the

standard deviation s_R only reduces reliability uncertainty, so, it reduces the consequential reliability decline.

The reliability index decreases from the value $\beta = 3.652$ to values $\beta = 2.754$ (I 400) and $\beta = 2.200$ (I 800) for the maximum crack given by limitations (29). This represents a significant reliability decline that for the administrator of the bridge may not be acceptable. If crack would no longer grow, the remaining lifetime of member in ultimate limit state is lower than 3 years according to works [1,47]. In the case of further crack growth, the remaining lifetime would be significantly reduced and it means that the member would become unreliable.

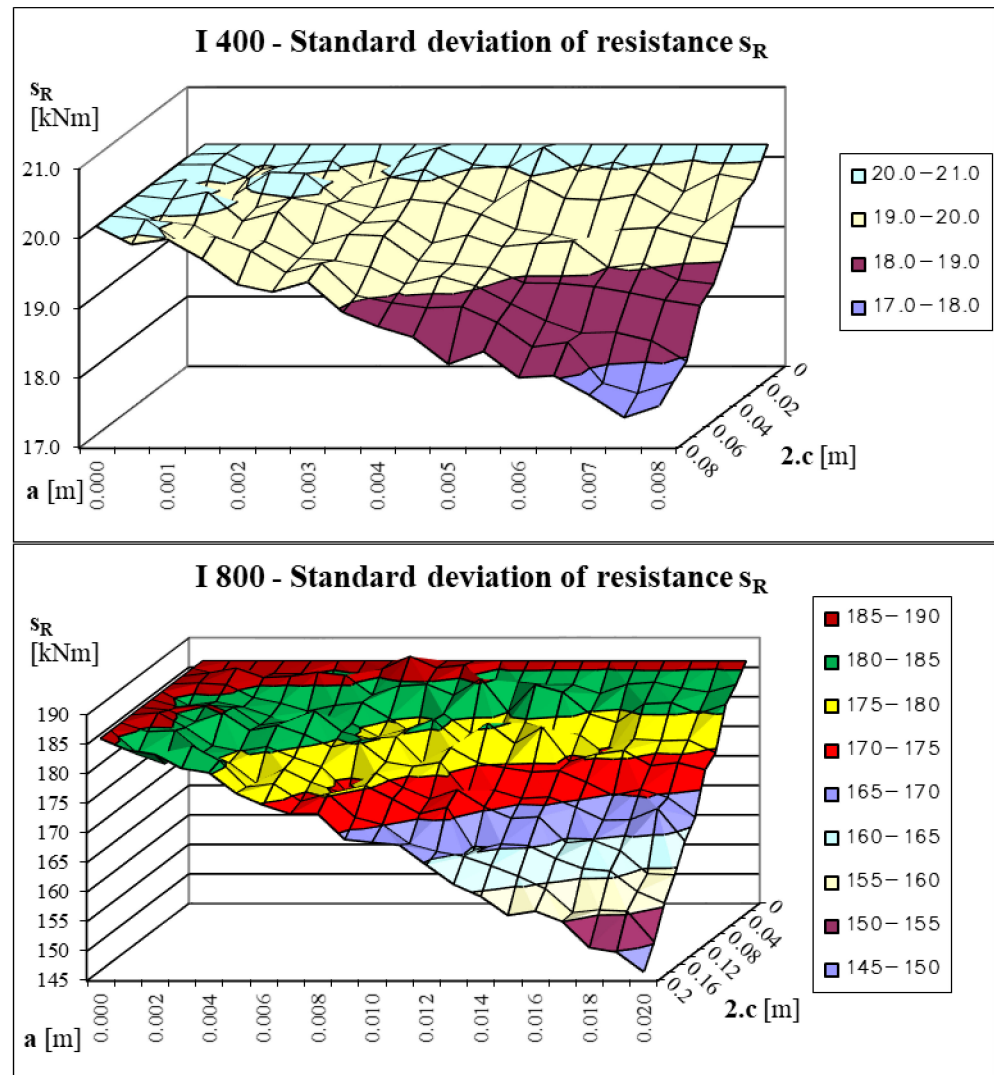


Figure 8. Influence of crack size on resistance standard deviation s_R .

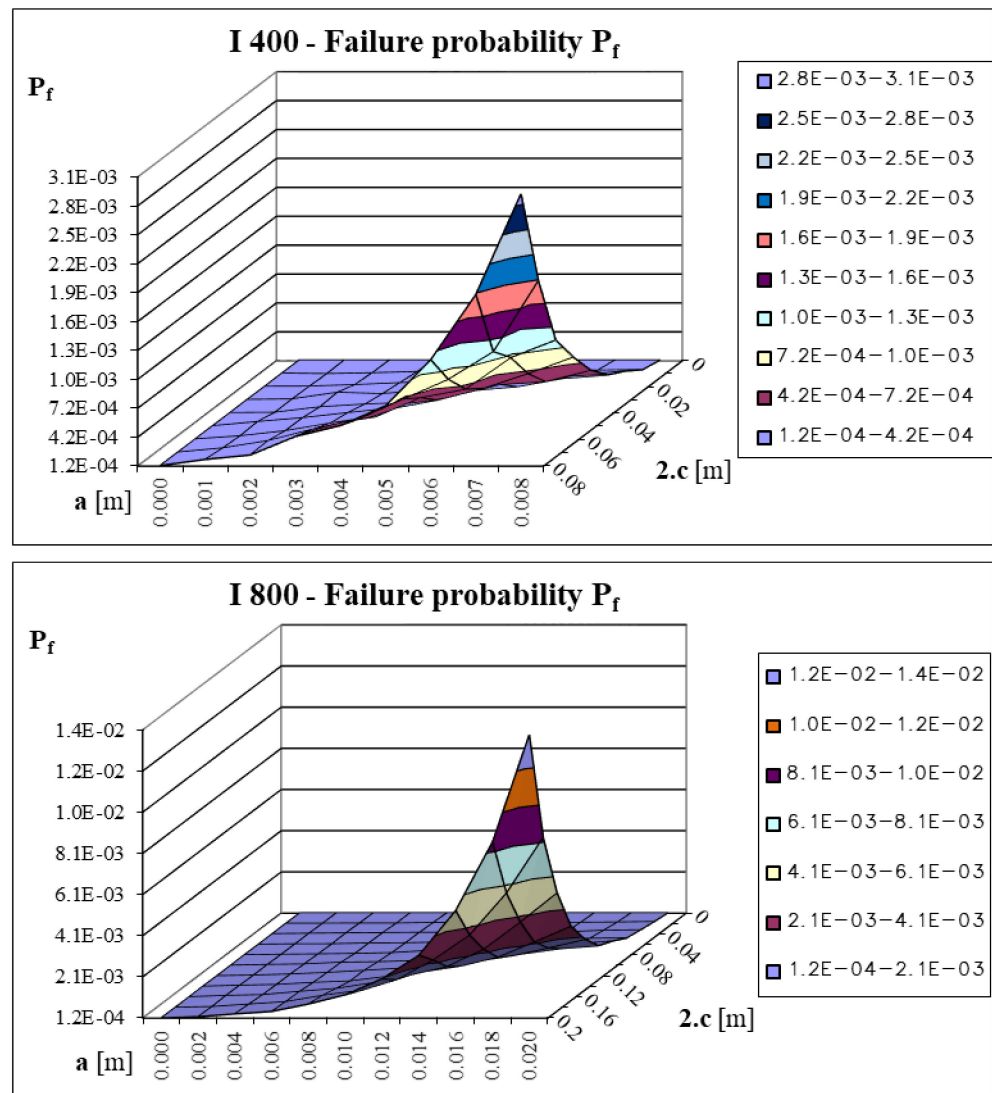


Figure 9. Influence of crack size on failure reliability P_f .

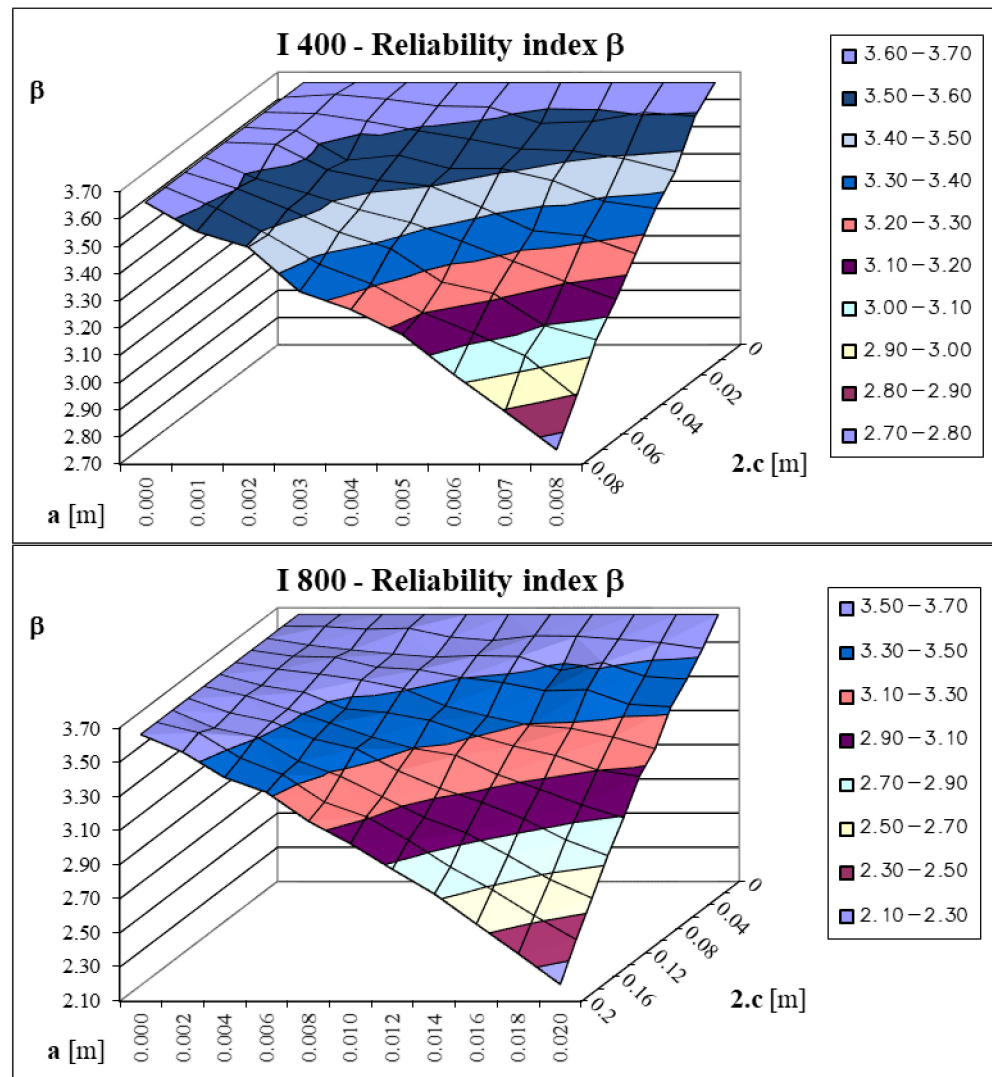


Figure 10. Influence of crack size on reliability index β .

7. Dependence of Crack Growth in Directions “a” and “c”

In fact, the crack growth in one direction depends on the crack growth in the other. Although this dependency was considered in several works such as [48–50], it has not yet been precisely defined.

Approach described in [51] was used for obtaining this dependency. For simplification, the crack growth is analysed at points (directions) “a” and “c” (in direction of main semi-axes). Crack propagation speed at those points is described by the stress-intensity factor (ΔK) and by the Paris-Erdogan law, which can be expressed as

$$\frac{da}{dN} = C \cdot (\Delta K_a)^m, \tag{30}$$

$$\frac{dc}{dN} = C \cdot (\Delta K_c)^m, \text{ respectively,} \tag{31}$$

where:

ΔK_a is the stress-intensity factor in direction “a”,
 ΔK_c is the stress-intensity factor in direction “c”,
 C, m are the material constants.

Relation between the crack depth increment Δa and the crack width increment Δc is obtained by combination of Equations (30) and (31)

$$\Delta a = \left(\frac{\Delta K_a}{\Delta K_c} \right)^m \cdot \Delta c. \quad (32)$$

The stress-intensity factor ΔK is in general given by Equation (17). Forms of SIF at points "a" and "c" are obtained from adjustment into increment form

$$\Delta K_a = F_a \cdot \sqrt{\frac{\pi \cdot a}{\Phi}} \cdot \Delta \sigma, \quad (33)$$

$$\Delta K_c = F_c \cdot \sqrt{\frac{\pi \cdot a}{\Phi}} \cdot \Delta \sigma. \quad (34)$$

The boundary-correction factor in general form, $F = F(a)$, is given by relation (9). Since the terms M_1, M_2, M_3 and thus the whole expression M in Equation (9) depend only on the ratios a/c and a/t , and do not depend on angle θ , then the value of the parameter M is the same at points "a" and "c" (independent on direction). Similarly, the parameter f_w , given by the Equation (16) for the calculation of the parameter S , is independent on the angle θ (on direction). However, the parameters g (14) and f_ϕ (15) depend, apart from ratios a/c and a/t also on angle θ , it means that they depend on the position. Then, the calibration functions for the points "a" and "c" follows from Equations

$$F_a = M \cdot S_a, \text{ at point a,} \quad (35)$$

$$F_c = M \cdot S_c, \text{ at point c.} \quad (36)$$

Substituting Equations (33)–(36) into Equation (32), the adjusted Equation can be obtained for calculation of increment Δa as

$$\Delta a = \left(\frac{S_a}{S_c} \right)^m \cdot \Delta c. \quad (37)$$

Adjusting and substituting Equations (14)–(16) into Equation (13), one obtains the following Equation for calculation S_a , where it is valid for $\frac{a}{c} \leq 1, \theta = 0$ (at point "a")

$$S_a = g_a \cdot f_a \cdot f_w = \left[\frac{1}{\cos\left(\frac{\pi \cdot c}{b} \cdot \left(\frac{a}{c}\right)^{0.5}\right)} \right]^{0.5}, \quad (38)$$

and for calculation S_c , one obtains Equation, where it is valid for $\frac{a}{c} \leq 1, \theta = \frac{\pi}{2}$ (at point "c")

$$S_c = g_c \cdot f_a \cdot f_w = \left[1.1 + 0.35 \cdot \left(\frac{a}{t}\right)^2 \right] \cdot \left(\frac{a}{c}\right)^{0.5} \cdot \left[\frac{1}{\cos\left(\frac{\pi \cdot c}{b} \cdot \left(\frac{a}{c}\right)^{0.5}\right)} \right]^{0.5}. \quad (39)$$

Substituting (38) and (39) into (37) and adjusting, the Equation for calculation of the crack depth increment Δa in terms of crack width increment Δc can be obtained as follows

$$\Delta a = \left[\frac{1}{\left[1.1 + 0.35 \cdot \left(\frac{a}{t}\right)^2 \right] \cdot \left(\frac{a}{c}\right)^{0.5}} \right]^m \cdot \Delta c. \quad (40)$$

There to proceed by iterative way for the calculation of the crack growth in both directions one must choose the initial crack size with initial dimensions "a" and "c", then the increment Δc is selected and using Equation (40), the corresponding increase of increment Δa can be calculated. New crack dimensions "a" and "c" are obtained so that the

increments Δc and Δa are added to previous dimensions. Again, choosing increment Δc (same as before) and calculating a new corresponding increase Δa , new crack dimensions can be calculated. Calculation of crack growth will be finished if none of the restrictions (29) is violated. An example of crack dimension calculation for flange thickness $t_f = t = 10$ mm is shown in Table 3 and the results are shown in Figure 11.

Table 3. Crack growth.

Δc [mm]	Δa [mm]	c [mm]	a [mm]	Crack Cross-Sectional Area A_{tr} [mm ²]
		0.00001 ≈ 0	0.00001 ≈ 0	≈ 0
0.1	0.075	0.1	0.075	0.01178
0.1	0.116	0.2	0.191	0.06000
0.1	0.080	0.3	0.271	0.12771
0.1	0.087	0.4	0.358	0.22494
0.1	0.089	0.5	0.447	0.35107

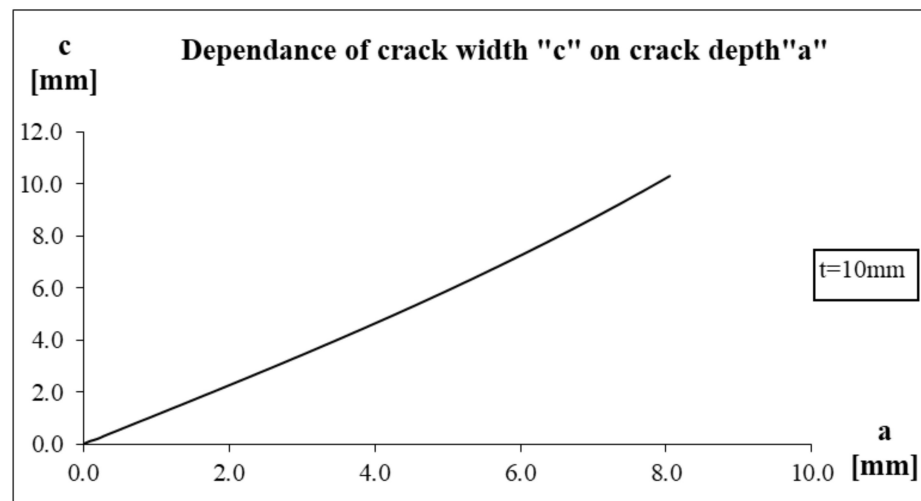


Figure 11. Influence of crack width “c” on crack depth “a”.

The initial ratio a/c (initial crack dimensions) is important for crack growth calculation in both directions. Basically, it is the minimum detectable crack. Since the minimum value of the measurable crack is not precisely defined (usually it is estimated) and similarly the ratio a/c is not known, the approach was intended for values close to zero (exact zero cannot be considered because of the ratio a/c). The work [29] is also concerned with this problem.

The results show that the increment Δa is gradually increasing unevenly at constant increment Δc .

It is possible to obtain the crack growth in both directions using the described approach. The curve was drawn through the obtained values based on finding the dependence of crack growth in direction “c” on crack growth in direction “a”. The second degree polynomial curve turned out to be the most preferred form

$$c = k_1 \cdot a^2 + k_2 \cdot a + k_3, \tag{41}$$

where k_i are coefficients.

It has been proven that the values of the coefficient k_i depend not only on the thickness t_f , but also on selected increment Δc . Therefore, the sensitivity analysis was performed,

which improved values of the coefficient k_i . Table 4 shows the k_i values depending on the selected increment Δc , wherein the thickness of the flange was assumed $t_f = t = 10$ mm.

Table 4. Dependence between “c” and “a” for thickness of flange $t_f = 10$ mm depending on increment Δc .

Selected Increment Δc [mm]	Dependence between “c” and “a”
$\Delta c = 0.5$ mm	$c = 0.03093 \cdot a^2 + 1.01255 \cdot a + 0.06696$
$\Delta c = 0.1$ mm	$c = 0.03030 \cdot a^2 + 1.01960 \cdot a + 0.06844$
$\Delta c = 0.05$ mm	$c = 0.03024 \cdot a^2 + 1.02015 \cdot a + 0.06903$
$\Delta c = 0.01$ mm	$c = 0.03025 \cdot a^2 + 1.02027 \cdot a + 0.06972$
$\Delta c = 0.005$ mm	$c = 0.03027 \cdot a^2 + 1.02017 \cdot a + 0.06993$
$\Delta c = 0.001$ mm	$c = 0.03027 \cdot a^2 + 1.02022 \cdot a + 0.06995$

It is assumed that the increment reduction is meaningless and the values of coefficients k_i are not significantly changed. Therefore, the dependency for $\Delta c = 0.001$ mm is considered to be sufficiently accurate.

Similarly, the parametric study was used for investigation of the coefficients k_i , which are valid to other flange thickness t_f . Dependencies are shown in Table 5.

Table 5. Relationships between “c” and “a” depending on various flange thickness t_f .

Flange Thickness $t = t_f$ [mm]	Dependence between “c” and “a”
$t_f = 10$ mm	$c = 0.03027 \cdot a^2 + 1.02022 \cdot a + 0.06995$
$t_f = 13$ mm	$c = 0.0232 \cdot a^2 + 1.0270 \cdot a + 0.0883$
$t_f = 20$ mm	$c = 0.0151 \cdot a^2 + 1.0202 \cdot a + 0.1381$
$t_f = 30$ mm	$c = 0.0101 \cdot a^2 + 1.0203 \cdot a + 0.2076$

If the dependency is established of “c” not only on “a”, but also on flange thickness $t = t_f$ in the approach, the universal dependency of the crack growth in direction “c” on direction “a” and on flange thickness t , is obtained in the form

$$c = \frac{0.3027}{t} \cdot a^2 + 1.0202 \cdot a + 0.00699 \cdot t. \quad (42)$$

Again, the parametric study with same steel welded I-beams I 400 and I 800, which were considered before, was performed. The characteristics are given in Table 2.

The achieved results of change of the mean value m_R and the standard deviation s_R are shown in Figures 12 and 13. As expected, the results again show a decrease of the mean value and the standard deviation, but in this case, the mean value m_R of resistance decreased more realistically for about 3.84% (I 400) (4.92% for I 800) and in the case of standard deviation s_R for about 2.93% (I 400) (5.45% for I 800). The given course of curves proves that it is a random stochastic process and the results were obtained by numerical simulation, which is the reason for the variance of values.

If the approach and Equations were projected into failure probability P_f and reliability index β (Figures 14 and 15), it was possible to see that the decrease of the reliability is not so significant. Initially, in the case of smaller crack sizes (“a”, “c”), random character of parameters has greater impact on the monitored variables as the crack growth (similarly to the mean value and standard deviation of resistance). Influence of the crack size became greater after ratio $a/t = (0.2\sim 0.3)$ was reached.

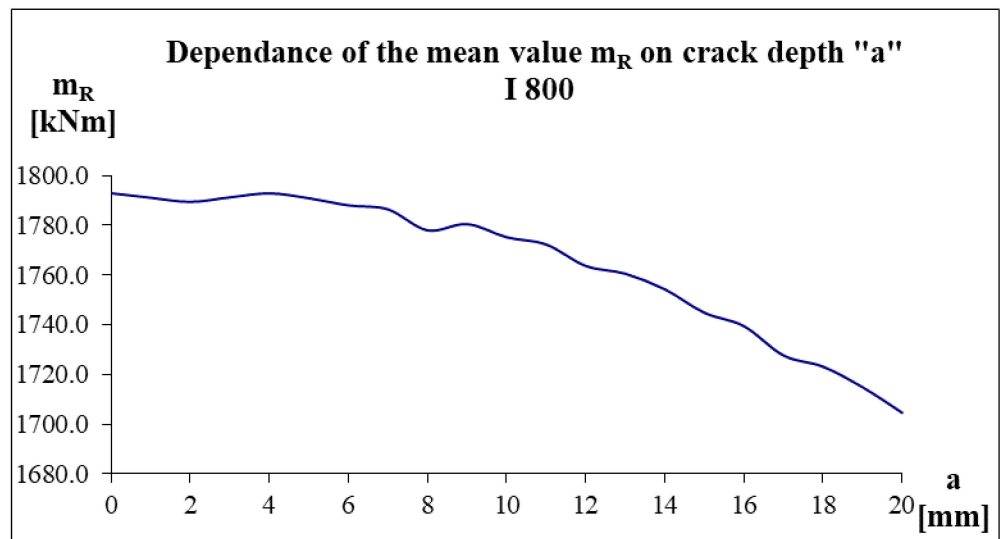
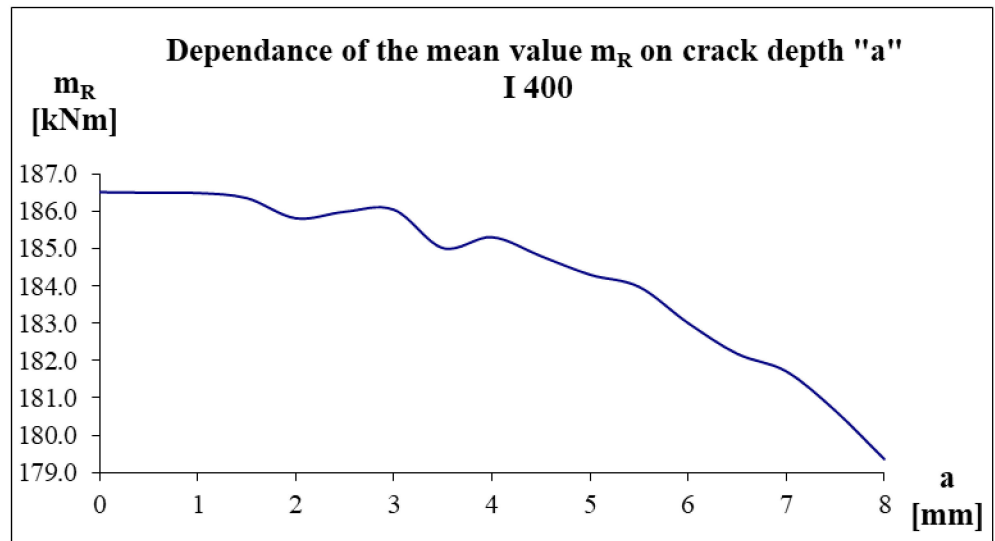


Figure 12. Dependence of resistance mean value m_R on crack depth "a".

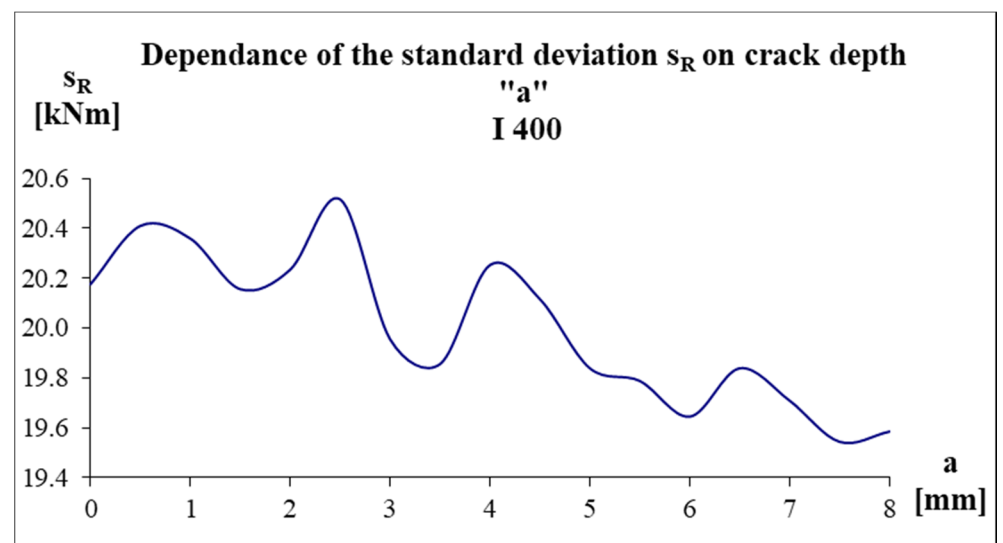


Figure 13. Cont.

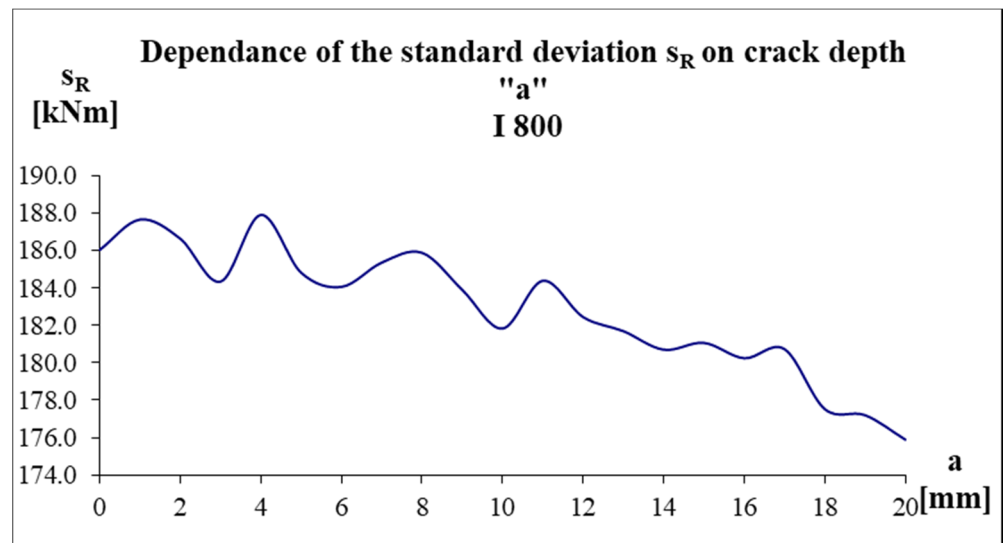


Figure 13. Dependence of resistance standard deviation s_R on crack depth "a".

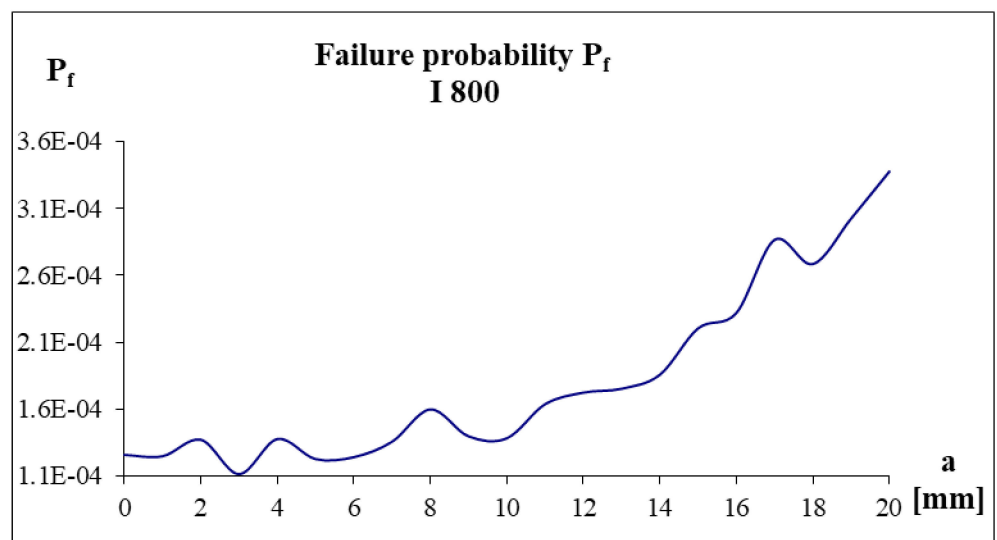
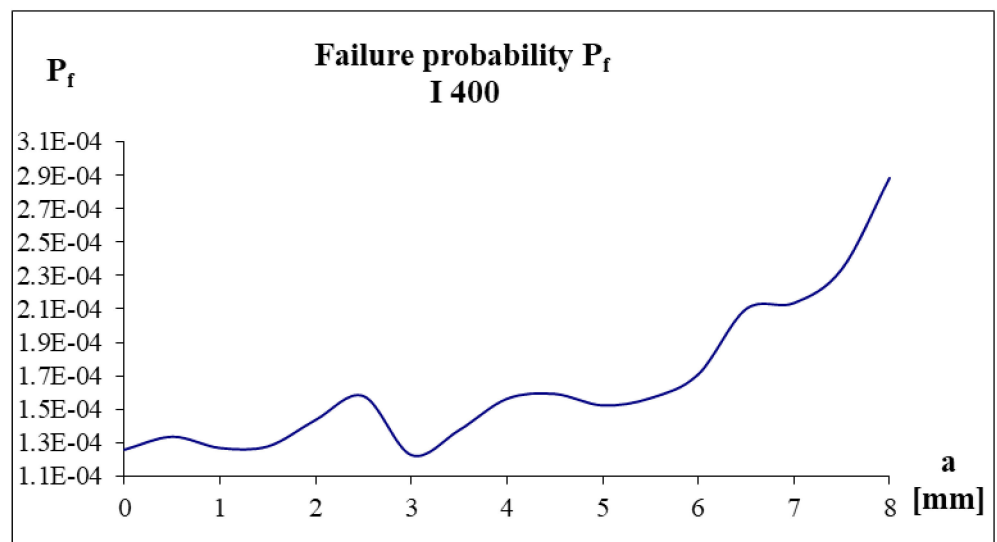


Figure 14. Dependence of failure probability P_f on crack depth "a".

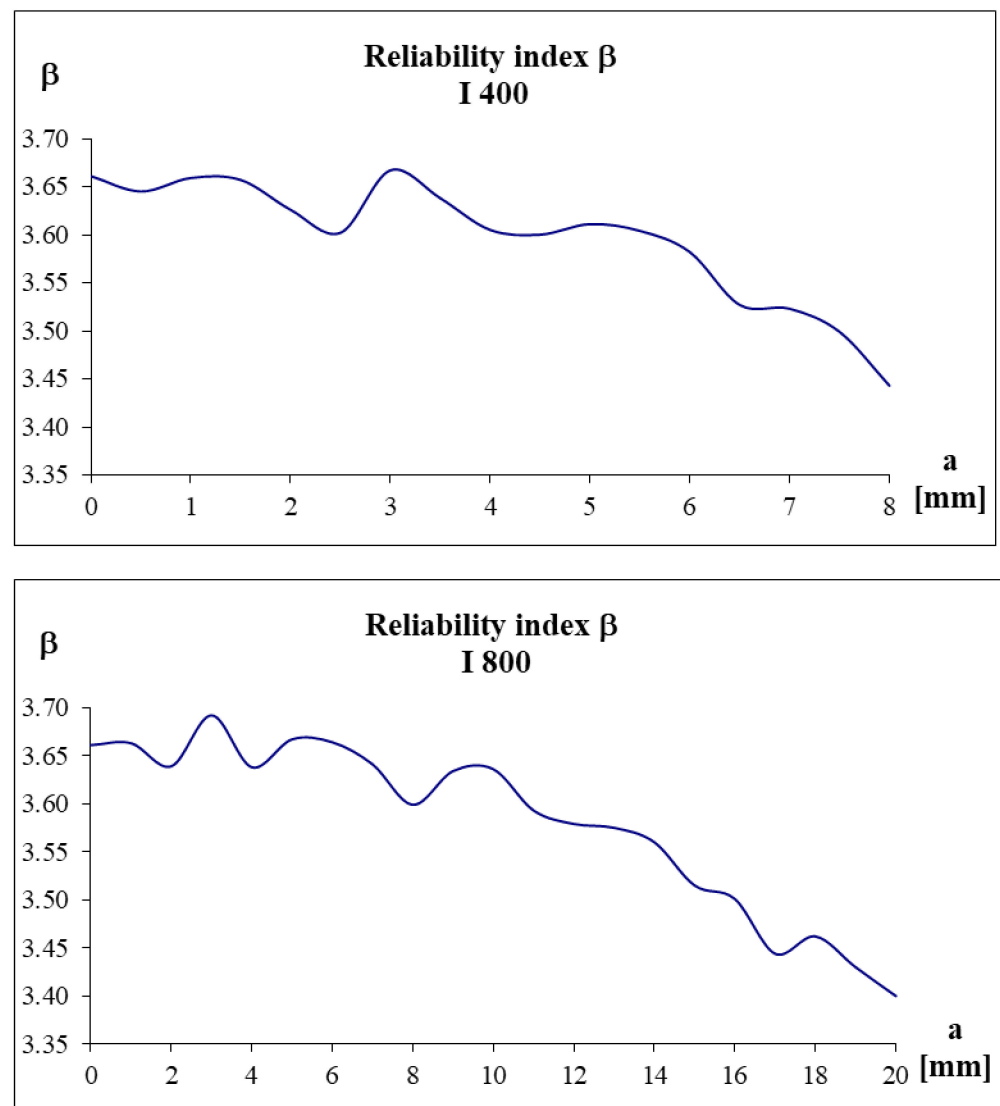


Figure 15. Dependence of reliability index β on crack depth “a”.

Reliability index β of the member at the maximum dimension of the considered crack $a = 0.8 \cdot t$ takes the values $\beta = 3.443$ (I 400) and $\beta = 3.400$ (I 800). It means that its remaining lifetime at ultimate limit state according to paper [47] is approximately 20–30 years depending on the age of member. Again, the course of the curves proves that this is a random stochastic process and the results were obtained by numerical simulation, which causes the variance of values.

8. Conclusions

The paper is focused on the influence of fatigue damage (fatigue cracks) of the steel welded I-girders on change of moment resistance and reliability in time. Methods such as analytical calculation and probabilistic calculation (numerical simulations) were used. The crack due to fatigue in tension flange of welded I-girder changes the cross-sectional characteristics as cross-sectional area, second moment of area and plastic or elastic section modulus. The analytical calculation and also probabilistic approach showed the following conclusions:

- In the case of independent crack growth in directions “a” and “c”, the fatigue crack can cause unavoidable decline of moment resistance (deterministic and stochastic) from the viewpoint of the Ultimate Limit States, what is going to decrease the member

- reliability from $\beta = 3.652$ to $\beta = 2.754$ (I400) and to $\beta = 2.200$ (I800) within bridge lifetime of 100 years.
- The derivation of the model of dependent crack growth in both directions represents a major contribution of this work. Using this approach, it is possible to directly determine the bending resistance and fatigue stressing from the viewpoint of the Ultimate Limit States.
 - In the case of dependent crack growth, the reliability index β of the member at the maximum dimension of the considered crack $a = 0.8 \cdot t$ takes the values of $\beta = 3.443$ (I 400) and $\beta = 3.400$ (I 800) respecting strength criteria of the Ultimate Limit States.
 - The results of the study showed more favourable and real (lower changes) interconnection between fatigue stressing and bending resistance. However, it still tends to decrease reliability of the member and to shorten the remaining lifetime.

Author Contributions: Conceptualization, P.K. and J.V.; data curation, P.K.; software, P.K.; validation, P.K. and J.V.; formal analysis, P.K. and J.V.; visualization, P.K.; writing—original draft preparation, P.K.; writing—review & editing, J.V.; All authors have read and agreed to the published version of the manuscript.

Funding: This research was supported by the Slovak Research and Development Agency under contract No. APVV-14-0772, and by Research Project No. 1/0306/21 and Project No. 1/0623/21 of the Slovak Grant Agency, and under the project of Operational Programme Interreg V-A Slovak Republic—Czech Republic: Assessment of the impact of the environmental load on the bridge structures condition of the cross-border transportation network, No. 304011Y277. The project is co-funding by European Regional Development Fund.

Institutional Review Board Statement: Not applicable.

Informed Consent Statement: Not applicable.

Data Availability Statement: Not applicable.

Conflicts of Interest: The authors declare no conflict of interest.

References

1. Kotes, P.; Vican, J. Recommended reliability levels for the evaluation of existing bridges according to Eurocodes. *Struct. Eng. Int.—Int. Assoc. Bridge Struct. Eng. (IABSE)* **2013**, *23*, 411–417.
2. Vican, J.; Gocal, J.; Odrobinak, J.; Moravcik, M.; Kotes, P. Determination of railway bridges loading capacity. *Procedia Eng.* **2015**, *111*, 839–844. [[CrossRef](#)]
3. Vican, J.; Gocal, J.; Odrobinak, J.; Kotes, P. Analysis of existing steel railway bridges. *Procedia Eng.* **2016**, *156*, 507–514. [[CrossRef](#)]
4. Nagesha, A.; Valsan, M.; Kannan, R.; Rao, K.B.S.; Mannan, S.L. Influence of temperature on the low cycle fatigue behaviour of a modified 9Cr-1Mo ferritic steel. *Int. J. Fatigue* **2002**, *24*, 1285–1293. [[CrossRef](#)]
5. Hirschberg, V.; Rodrigue, D. Fourier Transform (FT) Analysis of the Stress as a Tool to Follow the Fatigue Behavior of Metals. *Appl. Sci.* **2021**, *11*, 3549. [[CrossRef](#)]
6. Sakai, T.; Nakagawa, A.; Nakamura, Y.; Oguma, N. Proposal of a Probabilistic Model on Rotating Bending Fatigue Property of a Bearing Steel in a Very High Cycle Regime. *Appl. Sci.* **2021**, *11*, 2889. [[CrossRef](#)]
7. Mashayekhi, M.; Santini-Bell, E. Fatigue assessment of a complex welded steel bridge connection utilizing a three-dimensional multi-scale finite element model and hotspot stress method. *Eng. Struct.* **2020**, *214*, 110624. [[CrossRef](#)]
8. Zhu, Z.; Xiang, Z.; Li, J.; Huang, Y.; Ruan, S. Fatigue behavior of orthotropic bridge decks with two types of cutout geometry based on field monitoring and FEM analysis. *Eng. Struct.* **2020**, *209*, 109926. [[CrossRef](#)]
9. Zhang, W.; Yuan, H. Corrosion fatigue effects on life estimation of deteriorated bridges under vehicle impacts. *Eng. Struct.* **2014**, *71*, 128–136. [[CrossRef](#)]
10. Chun-Qing, L.; Wei, Y.; Wenhai, S. Corrosion effect of ferrous metals on degradation and remaining service life of infrastructure using pipe fracture as example. *Struct. Infrastruct. Eng.* **2020**, *16*, 583–598.
11. Li, H.; Wu, G. Fatigue Evaluation of Steel Bridge Details Integrating Multi-Scale Dynamic Analysis of Coupled Train-Track-Bridge System and Fracture Mechanics. *Appl. Sci.* **2020**, *10*, 3261. [[CrossRef](#)]
12. Cui, C.; Xu, Y.; Zhang, Q.; Wang, F. Vehicle-induced fatigue damage prognosis of orthotropic steel decks of cable-stayed bridges. *Eng. Struct.* **2020**, *212*, 110509. [[CrossRef](#)]
13. Guo, T.; Chen, Y.u. Fatigue reliability analysis of steel bridge details based on field-monitored data and linear elastic fracture mechanics. *Struct. Infrastruct. Eng.* **2013**, *9*, 496–505. [[CrossRef](#)]
14. Fageehi, Y.A. Two- and Three-Dimensional Numerical Investigation of the Influence of Holes on the Fatigue Crack Growth Path. *Appl. Sci.* **2021**, *11*, 7480. [[CrossRef](#)]

15. Helmerich, R.; Kühn, B.; Nussbaumer, A. Assessment of existing steel structures. A guideline for estimation of the remaining fatigue life. *Struct. Infrastruct. Eng.* **2007**, *3*, 245–255. [[CrossRef](#)]
16. Alvarez-Armas, I.; Krupp, U.; Balbi, M.; Herenu, S.; Marinelli, M.C.; Knobbe, H. Growth of short cracks during low and high cycle fatigue in a duplex stainless steel. *Int. J. Fatigue* **2012**, *41*, 95–100. [[CrossRef](#)]
17. Shrestha, S.; Kannan, M.; Morscher, G.N.; Presby, M.J.; Razavi, S.M. In-situ fatigue life analysis by modal acoustic emission, direct current potential drop and digital image correlation for steel. *Int. J. Fatigue* **2021**, *142*, 105924. [[CrossRef](#)]
18. Skoglund, O.; Leander, J.; Karoumi, R. Optimizing the steel girders in a high strength steel composite bridge. *Eng. Struct.* **2020**, *221*, 110981. [[CrossRef](#)]
19. Di, J.; Ruan, X.; Zhou, X.; Wang, J.; Peng, X. Fatigue assessment of orthotropic steel bridge decks based on strain monitoring data. *Eng. Struct.* **2021**, *228*, 111437. [[CrossRef](#)]
20. Yan, F.; Chen, W.; Lin, Z. Prediction of fatigue life of welded details in cable-stayed orthotropic steel deck bridges. *Eng. Struct.* **2016**, *127*, 344–358. [[CrossRef](#)]
21. Wang, W.; Deng, L.; Shao, X. Number of stress cycles for fatigue design of simply-supported steel I-girder bridges considering the dynamic effect of vehicle loading. *Eng. Struct.* **2016**, *110*, 70–78. [[CrossRef](#)]
22. Soares, B.; Luiz, H.; Modenesi, P.J.; Godefroid, L.B.; Arias, A.R. Fatigue crack growth rates on the weld metal of high heat input submerged arc welding. *Int. J. Fatigue* **2019**, *119*, 43–51.
23. Gadallah, R.; Tsutsumi, S.; Yonezawa, T.; Shimanuki, H. Residual stress measurement at the weld root of rib-to-deck welded joints in orthotropic steel bridge decks using the contour method. *Eng. Struct.* **2020**, *219*, 110946. [[CrossRef](#)]
24. European Union. *EN 1993-2 Eurocode 3. Design of Steel Structures. Part 2: Steel Bridges*; European Union: Brussels, Belgium, 2007.
25. European Union. *EN 1993-1-9 Eurocode 3. Design of Steel Structures. Part 1–9: Fatigue*; European Union: Brussels, Belgium, 2007.
26. Tomica, V.; Gocal, J.; Kotes, P. Acceptable size of fatigue crack on tension flange of steel bridges. In Proceedings of the Czech and Slovak International Conference, Bratislava, Slovakia, 25–26 April 2006; pp. 91–96.
27. Tomica, V. Key Dimensions of Fatigue Cracks in Steel Structures. In Proceedings of the 20th Czech-Slovak Conference with International Participation, Steel Structures and Bridges, Prague, Czech Republic, 17–20 September 2003; pp. 163–168. (In Czech).
28. Fisher, J.W.; Kulak, G.L.; Smith, I.F.C. *Fatigue Primer for Structural Engineering*; National Steel Bridge Alliance: Chicago, IL, USA, 1998.
29. Gocal, J. Application of Probabilistic Approach on Observation of Fatigue Crack Propagation Using Linear Elastic Fracture Mechanics. Ph.D. Thesis, University of Zilina, Zilina, Slovakia, June 2000. (In Slovak).
30. Gocal, J.; Vican, J.; Hlinka, R.; Jost, J. Laboratory tests of a typical fatigue prone riveted steel railway bridge structural detail. *Procedia Eng.* **2010**, *2*, 1761–1766. [[CrossRef](#)]
31. Zehnder, A.T. Stress Intensity Factors. In *Encyclopedia of Tribology*; Wang, Q.J., Chung, Y.W., Eds.; Springer: Boston, MA, USA, 2013.
32. Zhang, J.; Yang, W.; Chen, J.; Xu, R. Direct Evaluation of the Stress Intensity Factors for the Single and Multiple Crack Problems Using the P-Version Finite Element Method and Contour Integral Method. *Appl. Sci.* **2021**, *11*, 8111. [[CrossRef](#)]
33. Smith, C.W.; Peters, W.H.; Kirbi, G.C.; Andonian, A. Stress-intensity distribution for natural flaw shapes approximating “Benchmark” geometries. In Proceedings of the Thirteenth National Symposium on Fracture Mechanics “Fracture Mechanics”, Philadelphia, PA, USA, 16–18 June 1980; pp. 422–437.
34. Tomica, V.; Slavík, J. Fatigue reliability of existing steel structures. In *Studies of University of Transport and Communications in Žilina*; EDIS: Bratislava, Žilina, 1996.
35. Newman, J.C., Jr.; Raju, I.S. Stress-intensity factor equations for cracks in three-dimensional finite bodies. In Proceedings of the Fourteenth National Symposium on Fracture Mechanics “Fracture Mechanics”, Volume I—Theory and Analysis, Los Angeles, CA, USA, 30 June–2 July 1981; pp. 1-238–1-265.
36. Newman, J.C., Jr.; Raju, I.S. *Analyses of Surface Cracks in Finite Plates under Tension or Bending Loads*; NASA TP-1578; National Aeronautics and Space Administration: Washington, DC, USA, 1979.
37. Anderson, T.L. *Fracture Mechanics: Fundamentals and Applications*; CRC Press: Boca Raton, FL, USA, 2005; 611p.
38. Paris, P.C.; Gomez, M.P.; Anderson, W.E. A rational analytic theory of fatigue. *Trend Eng.* **1961**, *13*, 9–14.
39. Paris, P.C.; Erdogan, F. A critical analysis of crack propagation laws. *J. Basic Eng.* **1963**, *85*, 528–533. [[CrossRef](#)]
40. Bujnak, J.; Gocal, J.; Odrobinak, J. Potential modelling and verification of bridge superstructures behaviour, 9th International symposium on steel bridges. *IOP Conf. Ser. Mater. Sci. Eng.* **2018**, *419*, 012011. [[CrossRef](#)]
41. Odrobinak, J.; Hlinka, R. Degradation of steel footbridges with neglected inspection and maintenance. Bridges in Danube basin 2016—New trends in bridge engineering and efficient solution for large and medium span bridges. *Procedia Eng.* **2016**, *156*, 304–311.
42. Krejsa, M.; Koubova, L.; Flodr, J.; Protivinsky, J.; Nguyen, Q.T. Probabilistic prediction of fatigue damage based on linear fracture mechanics. *Frat. ed Integrita Strutt.* **2017**, *39*, 143–159. [[CrossRef](#)]
43. Kala, Z. Global Sensitivity Analysis of Reliability of Structural Bridge System. *Eng. Struct.* **2019**, *194*, 36–45. [[CrossRef](#)]
44. Kala, Z. Sensitivity Analysis in Probabilistic Structural Design: A Comparison of Selected Techniques. *Sustainability* **2020**, *12*, 4788. [[CrossRef](#)]
45. Mrazik, A. *Theory of Steel Structures Reliability*; VEDA: Bratislava, Slovakia, 1987; 360p. (In Slovak)
46. STN 73 2611 + Amendment 3—1993: *Ultimate Tolerances of Dimensions of Steel Structures*; Slovak Office of Standards, Metrology and Testing: Bratislava, Slovakia, 1993. (In Slovak)

47. Kotes, P.; Vican, J. Reliability levels for existing bridges evaluation according to Eurocodes. *Procedia Eng.* **2012**, *40*, 211–216. [[CrossRef](#)]
48. Tomica, V.; Slavik, J. *Effect of Inspection on Fatigue Life of Existing Orthotropic Steel Bridge Decks*; European Workshop “Thin-Walled Steel Structures”: Kreisau, Poland, 1996; pp. 167–174.
49. Tomica, V.; Hric, M. Shape of fatigue crack in flange-plate members. In Proceedings of the 17th Czech-Slovak International Conference “Steel Structures and Bridges”, Bratislava, Slovakia, 9 July–9 September 1994; pp. I-313–I-318.
50. Tomica, V. Assessment of crack-like imperfections in fillet welded attachments in orthotropic steel deck. In *Studies of University of Transport and Communications in Žilina*; EDIS: Bratislava, Žilina, 1995; Volume 18, pp. 15–27.
51. Jolles, M.; Tortoriello, V. Geometry variations during fatigue growth of surface flaws. In Proceedings of the Fourteenth National Symposium on Fracture Mechanics “Fracture Mechanics”, Volume I—Theory and Analysis, Los Angeles, CA, USA, 30 June–2 July 1981; pp. I-297–I-307.